

THE CO-EVOLUTION OF COSMIC ENTROPY AND STRUCTURES IN THE UNIVERSE

XINGHAI ZHAO^{1,2}, YUEXING LI^{1,2}, QIRONG ZHU^{1,2} AND DEREK FOX^{1,2}

¹Department of Astronomy and Astrophysics, The Pennsylvania State University, 525 Davey Lab, University Park, PA 16802, USA and

²Institute for Gravitation and the Cosmos, The Pennsylvania State University, 104 Davey Lab, University Park, PA 16802, USA

Draft version November 9, 2012

ABSTRACT

According to the second law of thermodynamics, the arrow of time points to an ever increasing entropy of the Universe. However, exactly how the entropy evolves with time and what drives the growth remain largely unknown. Here, for the first time, we quantify the evolving entropy of cosmic structures using a large-scale cosmological hydrodynamical simulation. Our simulation starts from initial conditions predicted by the leading Λ CDM cosmology, self-consistently evolves the dynamics of both dark and baryonic matter, star formation, black hole growth and feedback processes, from the cosmic dawn to the present day. Tracing the entropy contributions of these distinct components in the simulation, we find a strong link between entropy growth and structure formation. The entropy is dominated by that of the black holes in all epochs, and its evolution follows the same path as that of galaxies: it increases rapidly from a low-entropy state at high redshift until $z \sim 2$, then transits to a slower growth. Our results suggest that cosmic entropy may co-evolve with cosmic structure, and that its growth may be driven mainly by the formation of black holes in galaxies. We predict that the entropy will continue to increase in the near future, but likely at a constant rate.

Subject headings: galaxies: formation – galaxies: evolution — galaxies: halos — DM – cosmology: theory — entropy

1. INTRODUCTION

The “arrow of time” in our Universe, which has enabled its evolution to the present highly complex state, with large scale structure, galaxies, stars, and planetary systems – not to mention life itself – has its origins in the extremely low-entropy initial state of our cosmos (Penrose 1989; Carroll 2010), and barring unforeseen calamities, will persist for some 10^{100} years until the Universe achieves its equilibrium state, aka its “heat death” (Thomson 1852). Throughout this extremely long yet transient epoch, the probabilistic laws of Boltzmann’s statistical mechanics assure us, the entropy of the Universe will be always and ever increasing, as per the Second Law of Thermodynamics.

From this perspective, the formation and evolution of cosmic structure, as explored via large-scale cosmological surveys and numerical simulation, must also be always consistent with the Second Law. As such, both the initial formation and the subsequent evolution and (ultimately) dissolution of all the structures we observe must contribute to the ever-increasing entropy of the Universe.

Several studies (Basu & Lynden-Bell 1990; Frampton et al. 2009; Egan & Lineweaver 2010) have explored the entropy budget of the present-day observable Universe. These studies suggested that today’s total entropy is dominated by the entropy of the supermassive black holes (SMBHs) at the centers of galaxies. However, the detailed evolution of the entropy and its origin remain largely unknown.

Over the last several decades, numerical simulation have been very successful on the study of the evolution of the structures in the Universe from the time when the Universe was less than 1 million years old to the current time at 13.7 billion years later (e.g. Springel et al. (2005b)). They can also trace different energy forms in cosmic structures through vast scales, from dark matter (DM) in the large-scale structure to

gas and stars in the galaxies to ultra compact BHs while producing results that agree well with the astronomical observations. Thus numerical simulation is an ideal tool to study the evolution of the entropy along the cosmic structure formation.

In this paper, we present a quantitative study on the evolution of entropy using high-resolution cosmological hydrodynamical simulation. In § 2 we describe the numerical simulation, and the appropriate theoretical formulations for the entropy of different energy forms, using physical quantities that can be extracted directly from the simulation. In § 3, we present results of the formation and evolution of structures from the simulation, the evolution of cosmic entropy, and the link between entropy growth and structure formation. We summarize in § 4 the interpretations of the results and their implications.

2. METHODOLOGY

2.1. Numerical Simulation

Our cosmological simulation includes both dark and baryonic matter and related physical processes including star formation, BH growth, and feedback. It starts from initial conditions predicted by the leading cold dark matter cosmology, Λ CDM, and follows the formation and evolution of structures from redshift $z = 99$ to the current time at $z = 0$.

We performed the simulation using the parallel, N-body/SPH code GADGET-3, which is an improved version of the widely used simulation code GADGET (Springel et al. 2001b; Springel 2005). GADGET uses the “TreePM” method to compute gravitational forces, which combines a “tree” algorithm for short-range forces and a Fourier transform particle-mesh method for long-range forces. It incorporates an entropy-conserving formulation of SPH with adaptive particle smoothing. Radiative cooling and heating processes are calculated assuming collisional ionization equilibrium, and the UV background model of Faucher-Giguère et al. (2009) is used, which assumes that reionization was completed roughly by redshift $z \sim 6$.

Star formation is modeled in a multi-phase ISM, with a rate that follows the Schmidt-Kennicutt Law (Schmidt 1959; Kennicutt 1998). The model of BH growth and feedback follows that of Springel et al. (2005a) and Di Matteo et al. (2005), where the BH accretion is calculated using a spherical Bondi rate (Bondi 1952) under the Eddington limit, and its feedback is in form of thermal energy, $\sim 5\%$ of the radiation, injected into surrounding gas isotropically. We follow the seeding scheme of Zhu et al. (2012) and plant a seed of mass $M_{\text{BH}} = 10^5 \text{ h}^{-1} M_{\odot}$ in each halo once its total mass exceeds $10^{10} \text{ h}^{-1} M_{\odot}$, similar to previous cosmological simulations with BHs (Di Matteo et al. 2008, 2012). Such a self-regulated BH model has been demonstrated to successfully reproduce many observed properties of local galaxies (e.g., Di Matteo et al. 2005; Hopkins et al. 2006; Zhu et al. 2012) and the most distant quasars at $z \sim 6$ (Li et al. 2007).

The whole simulation is set up with a periodic boundary condition and the box size is 100 Mpc/h in comoving coordinates. The initial condition contains gas and DM components, each of them is represented by 512^3 particles with a gravitational softening length $\epsilon = 5 \text{ kpc/h}$. The cosmological parameters used are $\Omega_m = 0.27$, $\Omega_b = 0.045$, $\Omega_{\Lambda} = 0.73$ and $H_0 = 100 \text{ h km/s/Mpc}$ with $h = 0.7$, consistent with the seven-year results of the WMAP (Komatsu et al. 2011).

In order to identify structures formed on different scales, we use two on-the-fly group finding algorithms in the simulation. One is the friends-of-friends (FOF) algorithm used to link the DM particles with particle separations less than 0.2 times of the mean particle spacing. The gas, star and BH particles are then linked to the DM particle groups using the same algorithm. The other one is the SUBFIND algorithm (Springel et al. 2001a; Dolag et al. 2009) used to find gravitationally bound physical substructures in the groups. It first identifies the local overdensities using the SPH kernel interpolation, then the gravitationally unbound particles are iteratively removed. A substructure is considered physically bound if the final clumps have more than 20 particles. Throughout this work, a galaxy is defined as the group returned by the SUBFIND, which includes a DM halo, gas, stars, and BHs.

2.2. Entropy Formulation

We calculate the entropy of different energy forms of the Universe as follows: for gas and stars, we use the Sakur-Tetrode law (Basu & Lynden-Bell 1990; Egan & Lineweaver 2010),

$$S_i = kN_i \ln[Z_i(T)(2\pi m_i kT)^{\frac{3}{2}} e^{\frac{5}{2}} n_i^{-1} h^{-3}], \quad (1)$$

where N_i and Z_i represent the number of particles and internal partition function of either gas or star particles, n_i is the corresponding particle's number density and other symbols in Eq. (1) represent their normal physics quantities. For the gas particles, we take Z to be 1 for general baryonic matter. This is close to the value used in Basu & Lynden-Bell (1990), but we treat different types of the baryonic particles equally. All other quantities can be extracted from the numerical simulation. For the star particles, in principle, one should use different partition functions for different stellar populations. Because of the limitation of the resolution of the current cosmological simulation, it is not yet practical to trace the evolution of each stellar population directly. So we adopt the typical value of a main sequence star and the corresponding entropy per baryon for all star particles as calculated

in Basu & Lynden-Bell (1990). Since there is a simple relation between the entropy per baryon for gas and stars as used in Egan & Lineweaver (2010), here we use this relation and mass of the stellar component to estimate its entropy from the calculated gas entropy in the simulation.

For the entropy of DM in the Universe, it is worth noting that the nature of the DM particles is still unclear. Therefore, it is difficult to calculate the DM entropy in an exact way. In this study, we adopt the cold DM model and use a well-motivated definition from the studies of the X-ray clusters in astrophysics (Navarro et al. 1995; Eke et al. 1998; Faltenbacher et al. 2007). That is, we define the “temperature” of a DM particle via relation,

$$3kT = \mu m_p \sigma^2, \quad (2)$$

where μ is the mean molecular weight of the DM particle, m_p is the proton mass and σ is the three-dimensional velocity dispersion of the DM particle. σ can be easily extracted from numerical simulation while μ is a parameter that must be constrained from current investigations of the nature of the DM particles. Here, we adopt a typical value of 40 GeV for the mass of the DM particles from recent studies of weakly interacting massive particles (WIMP) (Geringer-Sameth & Koushiappas 2011). Now that we have a definition of the “temperature” of a DM particle, we can use Eq. (1) to calculate the entropy of the DM component in a way similar to that of the gas component in the simulation. We want to emphasize that this method is only to estimate the DM entropy from an astrophysics perspective.

To calculate the entropy of BHs, we use the Bekenstein-Hawking formula (Bekenstein 1973; Hawking 1976),

$$S_{\text{BH}} = \frac{kc^3 A}{4G\hbar}, \quad (3)$$

where A is the surface area of a BH. For simplicity, we treat the BHs in the simulation as non-rotating charge-free Schwarzschild BHs. So the surface area of the BHs can be calculated as $A = 16\pi G^2 M^2 / c^4$, where M is the BH mass. Then the entropy of a BH particle in the simulation can be calculated as,

$$S_{\text{BH}} = k \frac{4\pi G}{c\hbar} M^2. \quad (4)$$

As we can see from Eq. (4), the BH entropy is proportional to the square of its mass. This leads to a BH entropy dominant era in the cosmic evolution as we will illustrate in our results. But we need to keep in mind that the derivation of the BH entropy is not from the same origin as that of gas, star and DM. Its exact physical interpretation is still a matter of debate.

3. RESULTS

3.1. Formation and Evolution of Cosmic Structures

Owing to the formation of structures, the Universe evolves from a nearly homogeneous distribution of matter to a filamentary complex, the cosmic webs, with time, as demonstrated in Figure 1. Dense regions build up gradually along the filaments due to density fluctuation and gravitational instability, DM and gas in these regions collapse to form galaxies. These galaxies interact with each other and merge hierarchically to form ever larger ones. The BHs form in these massive halos, and they grow through gas accretion and mergers following the hierarchical buildup of their host galaxies. At high redshifts ($z \gtrsim 10$), the gas and DM are the dominant components, but stars and BHs form rapidly at later time ($z < 10$).

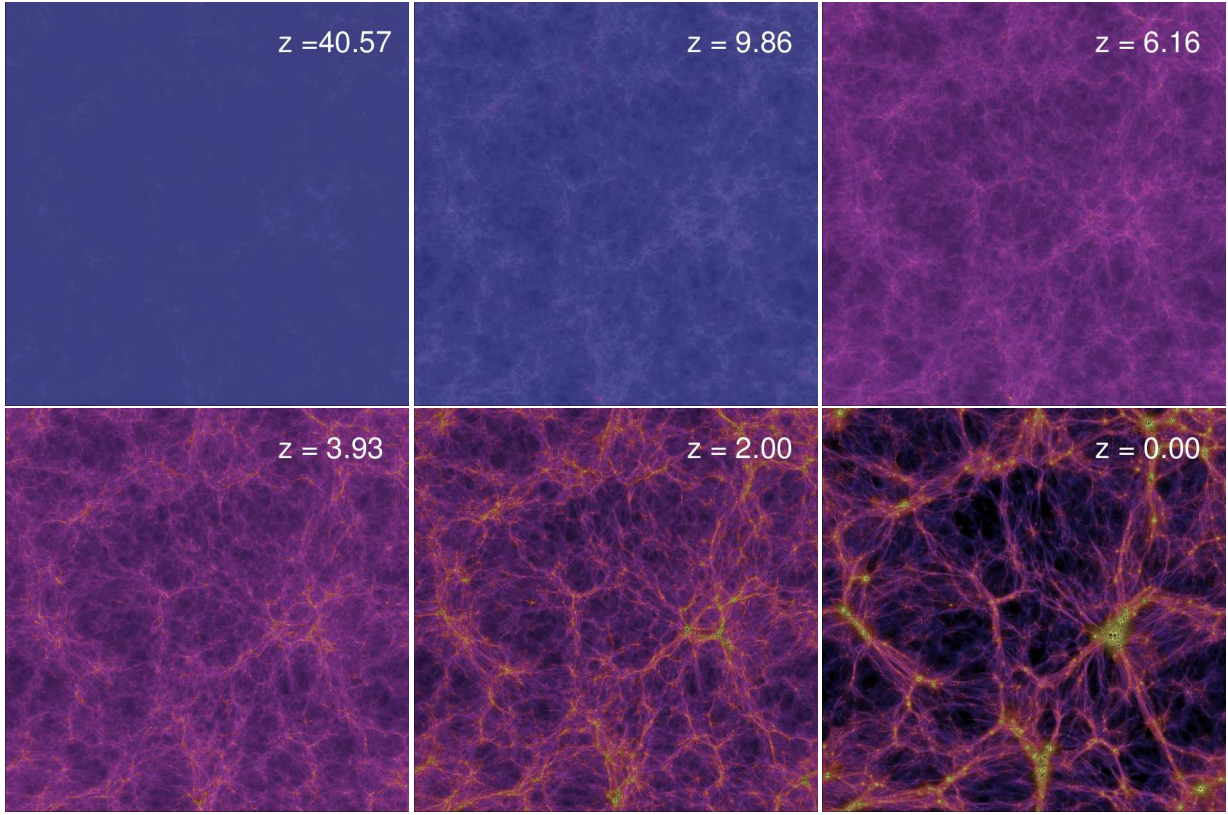


Figure 1. Formation and evolution of structures from the cosmological simulation. The images show the 2-D projected density of both gas and stellar components in a spatial slice in Z direction with a thickness of 10 Mpc/h (comoving). For the gas and stars, the brightness corresponds to the density while the color corresponds to the temperature of the gas (blue indicates cold gas, brown indicates hot, tenuous gas) and the metallicity of the stars (in yellow color). The BHs are represented by the black dots, the size of which is proportional to the BH mass. The box size is $100 h^{-1} \text{Mpc}$ in comoving coordinates.

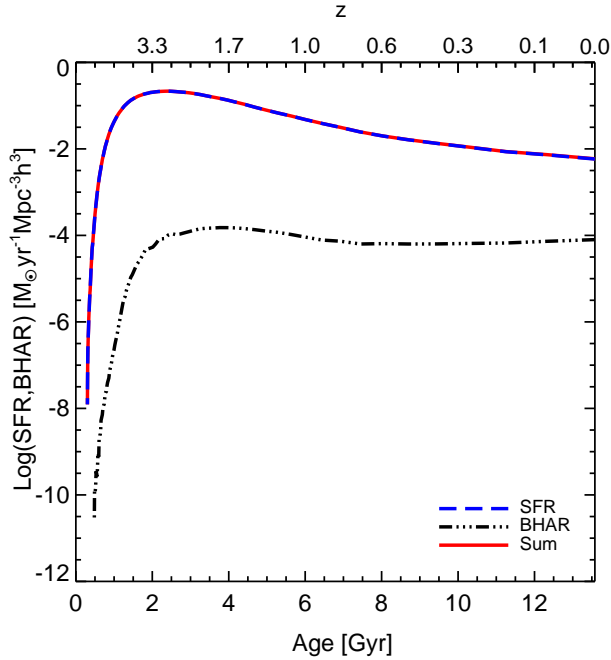


Figure 2. The growth history of structures from the simulation, as indicated by the density of the star formation rate (blue line), the BH accretion rate (black line), and their sum (red line) as a function of time.

The growth history of galaxies and BHs are shown in Figure 2. The star formation rate (SFR) rises sharply about 0.5 Gyrs ($z \sim 10$) after the Big Bang, it reaches its peak at around 2 Gyr ($z \sim 3$), then declines gradually with time. The BH accretion lags behind the star formation slightly, but it shares similar trend. It increases rapidly to its peak at $z \sim 2$, after that it decreases slowly and maintains a constant rate at late time. As a result of such growth, the accumulated mass of the galaxies, stars, and BHs increase monotonically with time. The BH accretion is about two to three orders of magnitude lower than the SFR, which may explain the tight correlation between the masses of the SMBHs and the stellar masses of their host galaxies, $M_{\text{BH}} \sim 10^{-2} - 10^{-3} M_*$ observed in nearby galaxies (Magorrian et al. 1998; Häring & Rix 2004).

Figure 2 clearly shows that the growth of the cosmic structure is driven by star formation at early time and BH formation at late time. The similarity between the star formation and BH growth indicates a co-evolution between galaxies and BHs.

3.2. Evolution of Cosmic Entropy

Using the formulation described in Sec. 2.2, we calculate the evolution history of the entropy of different energy forms in the observable Universe from redshift $z = 41$ to $z = 0$. In order to calculate the entropy of the whole observable universe, we first calculate it using our simulation data with a simulation box size of 100 Mpc/h and then scale this result up to the size of the observable universe with a typical value of 14.3 Gpc in radius (Cornish et al. 2004; Key et al. 2007; Egan & Lineweaver 2010; Bielewicz & Banday 2011) using the fact that the Universe is very close to uniform on the

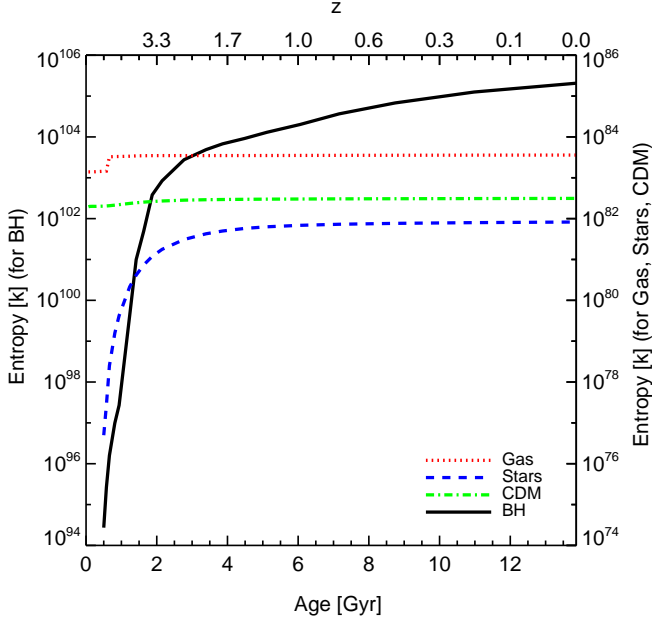


Figure 3. The evolution history of the entropy of the gas, stars, DM and BHs in the Universe. Note the different scales on the left and right axes. The left y-axis corresponds to the BH entropy, while the right y-axis corresponds to the gas, star and DM entropy.

scales larger than 100 Mpc/h. The resulting entropy of different structure components are shown in Figure 3.

For gas (baryonic matter), the entropy only has a very slight increase in the redshift range studied except a jump at redshift $8 < z < 9$ because of the cosmic reionization that is implemented in the simulation. The cosmic entropy at present day in this study is, however, about one magnitude higher than the estimation in Egan & Lineweaver (2010) as shown in Table 1. We believe this is caused by the fact that we can calculate the temperature of individual gas particles in the simulation while Egan & Lineweaver (2010) only uses the estimation of the whole gas component. Thus, our calculation is likely to be more accurate than the previous studies.

For the entropy of the stellar component, since it is calculated by scaling the entropy of the gas with their relative mass ratio, its present day value is also higher than the one in the previous studies (Egan & Lineweaver 2010). But, unlike the gas component, the stellar component's entropy increases dramatically once stars form in the simulation until redshift $z \sim 2$. Then it gradually increases to the present day's value. This is due to the rapid cosmic star formation before $z \sim 2$.

For the entropy of the DM, the way we calculate the entropy is different from the one in Egan & Lineweaver (2010) in which the relativistic degrees of freedom is used. So it is not straightforward to make a comparison in this case. Similar to the gas entropy, the DM entropy also increases slightly during the structure formation process.

For the entropy of the BHs, due to the limitation of the resolution of the simulation, we can only include the BHs with masses larger than $10^5 h^{-1} M_{\odot}$. So the BH entropy value we calculate in this study corresponds to the entropy of the SMBHs in Egan & Lineweaver (2010). Taking account that there are likely more BHs with masses close to $10^5 M_{\odot}$ in nature, the actual value of the BH entropy may be even higher.

The resulting entropy of BHs is at least more than 20 orders

Table 1

A comparison of different estimates of entropy of different energy forms in the present-day observable universe.

Energy form	Entropy (this study) [k]	Entropy (previous studies) ^a [k]
BHs	2.06×10^{105}	10^{106} [1], 10^{102} [2]
Gas	3.60×10^{83}	10^{82} [1]
Stars	8.25×10^{81}	10^{81} [1], 10^{79} [2]
CDM	3.13×10^{82}	$_{-b}$

^a [1] Egan & Lineweaver (2010), [2] Frampton et al. (2009)

^b The way we calculate the entropy is different from the one in Egan & Lineweaver (2010) in which the relativistic degrees of freedom is used. So it is not straightforward to make a comparison in this case.

of magnitude higher than the other energy forms throughout the cosmic time in Figure 3. Therefore, the total entropy of the Universe is dominated by that of the BHs. This is consistent with conclusions from previous studies for the present-day Universe (Basu & Lynden-Bell 1990; Frampton et al. 2009; Egan & Lineweaver 2010).

Table 1 gives a comparison of the different estimates of the entropy of different energy forms in the local observable universe. It shows that our simulation results are close to those from previous studies.

From Figure 3, we clearly see that the growth of the cosmic entropy is not a simple linear curve. It increases rapidly from a low-entropy state after the Big Bang until $z \sim 2$, then transits to a slower growth. Unlike the entropies of the stars and gas which only shows significant increase at early time but flattens at later times, the entropy of the BHs keeps increasing with time. This trend is likely to continue in the near future.

3.3. Structure Formation as Driver of Entropy Growth

The evolution of entropy in Figure 3 and the structure formation history in Figure 2 show a strikingly similar trend, as both increase rapidly at about the same time. This hints a possible link between the two.

To investigate the link between entropy and structure formation, we plot the growth rate of entropy as a function of time, in comparison with the SFR and BH accretion rate, as shown in Figure 4. It clearly shows that the generation of entropy is closely related to the SFR and the BH accretion rate over the redshift range studied. This coincidence suggests that cosmic entropy growth is driven by structure formation.

4. CONCLUSION

We have used a large-scale cosmological simulation to study the evolution history of the cosmic entropy along the structure formation in the Universe. Our calculations are based on well-motivated physical formulations using parameters directly from the simulation. Our estimations of the entropy of different energy forms in the local observable Universe are in broad agreement with previous studies.

Moreover, by tracking the evolution of entropy of different energy forms, we find that the entropy of BHs is at least 20 orders of magnitude higher than the other components including gas, stars and DM. Therefore, the cosmic entropy is dominated by that of the BHs. Rather than follow a simple linear curve, it has roughly two distinctive growth phases: a rapid increases phase from a low-entropy state at high redshift until $z \sim 2$, then transits to a slower growth phase.

Furthermore, we find a strikingly similar evolution between the growth rate of entropy and that of galaxies. This suggests

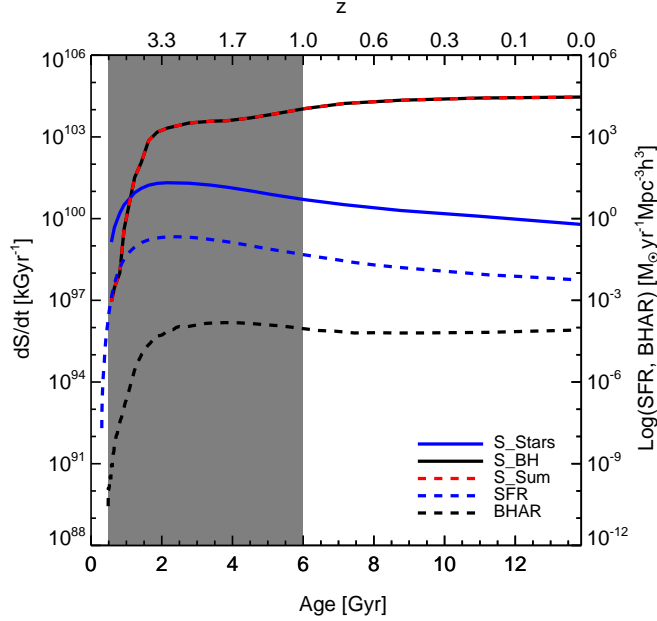


Figure 4. The evolution history of the entropy growth rate of BHs (black solid line), stars (blue solid line), and their sum (red dashed line), contrasted by the star formation rate (blue dashed line) and BH accretion rate (black dashed line). Note the difference in the y-axes. The left y-axis corresponds to the entropy growth rate, while the right y-axis corresponds to the structure growth rates. The shaded region indicates the period during which the entropy and structure grow rapidly and simultaneously.

that the cosmic entropy co-evolves with cosmic structures, and that generation of cosmic entropy is driven by structure formation in the Universe. We predict that the BH entropy, and hence the cosmic entropy, will continue to increase in the near future at a constant rate.

We note that due to the limitation of the resolution of the simulation, we can only include the BHs with masses larger than $10^5 h^{-1} M_{\odot}$. Taking into account smaller BHs may increase the actual value of the BH entropy. In addition, due to the unknown nature of DM, our calculation of its entropy may be subject to a large uncertainty. Nevertheless, these uncertainties would not affect our conclusion that the structure formation is the main driving force in the generation and evolution of the cosmic entropy.

ACKNOWLEDGMENTS

Support from NSF grants AST-0965694 and AST-1009867 is gratefully acknowledged. We acknowledge the Research Computing and Cyberinfrastructure unit of Information Technology Services at the Pennsylvania State University for providing computational resources and services that have contributed to the research results reported in this paper (URL: <http://rcc.its.psu.edu>). The Institute for Gravitation and the Cosmos is supported by the Eberly College of Science and

the Office of the Senior Vice President for Research at the Pennsylvania State University.

REFERENCES

- Basu, B., & Lynden-Bell, D. 1990, *QJRAS*, 31, 359
 Bekenstein, J. D. 1973, *Phys. Rev. D*, 7, 2333
 Bielewicz, P., & Banday, A. J. 2011, *MNRAS*, 412, 2104
 Bondi, H. 1952, *MNRAS*, 112, 195
 Carroll, S. M. 2010, *From Eternity to Here: The Quest for the Ultimate Theory of Time*
 Cornish, N. J., Spergel, D. N., Starkman, G. D., & Komatsu, E. 2004, *Physical Review Letters*, 92, 201302
 Di Matteo, T., Colberg, J., Springel, V., Hernquist, L., & Sijacki, D. 2008, *ApJ*, 676, 33
 Di Matteo, T., Khandai, N., DeGraf, C., Feng, Y., Croft, R. A. C., Lopez, J., & Springel, V. 2012, *ApJ*, 745, L29
 Di Matteo, T., Springel, V., & Hernquist, L. 2005, *Nature*, 433, 604
 Dolag, K., Borgani, S., Murante, G., & Springel, V. 2009, *MNRAS*, 399, 497
 Egan, C. A., & Lineweaver, C. H. 2010, *ApJ*, 710, 1825
 Eke, V. R., Navarro, J. F., & Frenk, C. S. 1998, *ApJ*, 503, 569
 Faltenbacher, A., Hoffman, Y., Gottlöber, S., & Yepes, G. 2007, *MNRAS*, 376, 1327
 Faucher-Giguère, C., Lidz, A., Zaldarriaga, M., & Hernquist, L. 2009, *ApJ*, 703, 1416
 Frampton, P. H., Hsu, S. D. H., Kephart, T. W., & Reeb, D. 2009, *Classical and Quantum Gravity*, 26, 145005
 Geringer-Sameth, A., & Koushiappas, S. M. 2011, *Physical Review Letters*, 107, 241303
 Häring, N., & Rix, H. 2004, *ApJ*, 604, L89
 Hawking, S. W. 1976, *Phys. Rev. D*, 13, 191
 Hopkins, P. F., Hernquist, L., Cox, T. J., Di Matteo, T., Robertson, B., & Springel, V. 2006, *ApJS*, 163, 1
 Kennicutt, Jr., R. C. 1998, *ApJ*, 498, 541
 Key, J. S., Cornish, N. J., Spergel, D. N., & Starkman, G. D. 2007, *Phys. Rev. D*, 75, 084034
 Komatsu, E., Smith, K. M., Dunkley, J., Bennett, C. L., Gold, B., Hinshaw, G., Jarosik, N., Larson, D., Nolte, M. R., Page, L., Spergel, D. N., Halpern, M., Hill, R. S., Kogut, A., Limon, M., Meyer, S. S., Odegard, N., Tucker, G. S., Weiland, J. L., Wollack, E., & Wright, E. L. 2011, *ApJS*, 192, 18
 Li, Y., Hernquist, L., Robertson, B., Cox, T. J., Hopkins, P. F., Springel, V., Gao, L., Di Matteo, T., Zentner, A. R., Jenkins, A., & Yoshida, N. 2007, *ApJ*, 665, 187
 Magorrian, J., Tremaine, S., Richstone, D., Bender, R., Bower, G., Dressler, A., Faber, S. M., Gebhardt, K., Green, R., Grillmair, C., Kormendy, J., & Lauer, T. 1998, *AJ*, 115, 2285
 Navarro, J. F., Frenk, C. S., & White, S. D. M. 1995, *MNRAS*, 275, 720
 Penrose, R. 1989, *The emperor's new mind. Concerning computers, minds and laws of physics*
 Schmidt, M. 1959, *ApJ*, 129, 243
 Springel, V. 2005, *MNRAS*, 364, 1105
 Springel, V., Di Matteo, T., & Hernquist, L. 2005a, *MNRAS*, 361, 776
 Springel, V., White, S. D. M., Jenkins, A., Frenk, C. S., Yoshida, N., Gao, L., Navarro, J., Thacker, R., Croton, D., Helly, J., Peacock, J. A., Cole, S., Thomas, P., Couchman, H., Evrard, A., Colberg, J., & Pearce, F. 2005b, *Nature*, 435, 629
 Springel, V., White, S. D. M., Tormen, G., & Kauffmann, G. 2001a, *MNRAS*, 328, 726
 Springel, V., Yoshida, N., & White, S. D. M. 2001b, *New Astronomy*, 6, 79
 Thomson, W. 1852, *On a Universal Tendency in Nature to the Dissipation of Mechanical Energy*, *Proceedings of the Royal Society of Edinburgh*
 Zhu, Q., Li, Y., & Sherman, S. 2012, *ArXiv e-prints* 1211.0013